SPACE WEATHER, VOL. 6, S09001, doi:10.1029/2008SW000406, 2008

Man-made space weather

Michael Mendillo,[1] Steven Smith,[1] Anthea Coster,[2] Philip Erickson,[2] Jeffrey Baumgardner,[1] and Carlos Martinis[1]

Received 21 April 2008; accepted 21 May 2008; published 11 September 2008.

[1] Major geomagnetic storms produce dramatic gradients in the ionosphere's total electron content (TEC) that cause errors in GPS-dependent navigation systems, such as those used by the U. S. Coast Guard and the Federal Aviation Administration. Here we describe the first use of GPS signals to detect large-scale gradients in TEC very similar to those found during ionospheric storms but produced instead by the exhaust gases of a large Titan rocket launched from the Kennedy Space Center. The severe ionospheric perturbations of 30 April 2005, observed simultaneously by optical emission from the thermosphere and by GPS diagnostics of the ionosphere, describe a unique type of space weather effect caused by nonnatural sources.

Citation: Mendillo, M., S. Smith, A. Coster, P. Erickson, J. Baumgardner, and C. Martinis (2008), Man-made space weather, *Space Weather*, *6*, S09001, doi:10.1029/2008SW000406.

1. Introduction

[2] Many services now require high precision navigation and positioning information on a routine and real-time basis. Examples include marine navigation, in-vehicle navigation systems, railway control, highway traffic management, emergency response, and commercial aviation. Large spatial gradients in the ionosphere's total electron content (TEC) introduce errors into positioning and navigation systems relying on the Global Positioning System (GPS). Thus, the optimal use of GPS capabilities across the continental United States (CONUS) occurs when spatial gradients in TEC are minimal. In the navigation solution, range errors due to the ionospheric group path delay of the GPS signals from multiple satellite directions depend on the slant TECs along each raypath. In quiet conditions, as described above, the slant TECs have a simple geometrical dependence upon the region's vertical TEC, as given by the secant of the raypath zenith angles from the receiving station. While the assumption of an equivalent uniform horizontal slab model of ionospheric TEC is not always accurate, departures have a known occurrence pattern. For example, near sunrise and sunset, gradients are known to occur in the east-west direction, and at night the TEC at midlatitudes can have appreciable gradients in the south-north direction. Thus, under geomagnetically quiet conditions, extra care can be used during these times and locations of known sources of variability.

[3] During periods of large geomagnetic storms, remarkable gradients in TEC can occur across CONUS, and these represent the greatest challenge to the use of GPS systems for precise navigation. Strong variations in the spatial locations of the TEC positive phase during ionospheric storms were observed for the first time by *Klobuchar et al.* [1971] and subsequent measurements showed them to have a regular pattern [*Mendillo and Klobuchar*, 1975] that could serve as a predictive aid [*Davies*, 1981]. The end of the TEC positive phase at a fixed location often occurs over short temporal and spatial scales, and such steep gradients can be readily observed in slant-integrated TEC measurements [*Mendillo et al.*, 1974]. In the GPS era, time-dependent maps of ionospheric storm enhanced densities (SEDs) were first described by *Coster et al.* [2001, 2003]. It soon became apparent that such coherent storm-time patterns offered the possibility of real-time specifications of SED locations and magnitudes to federal agencies. While the SED effect presents a strong enhancement for GPS to contend with, its spatial extent is large and its orientation from southeast to northwest is well known [*Mendillo and Klobuchar*, 1975; *Davies*, 1981; *Foster and Rideout*, 2005; *Mendillo and Klobuchar*, 2006]. However, the rapid termination of an SED's effect at a fixed location results in a far more confined spatial gradient, and this presents more serious concerns to forecasters. In the FAA study by Dehel et al. [2004], dynamical ''walls of depletion'' were described that could have as much as 84 TEC units change within 100 s, corresponding to 14 m of ionospherically imposed error suddenly occurring at a fixed location. The abrupt terminations of the TEC positive phase events studied by *Mendillo et al.* [1974] had depletion patterns ranging from 30 TEC units in 15 min to 50 TEC units over 2.5 h.

[4] Far less frequent than SEDs, but equally dramatic, are the TEC gradients caused by human spaceflight activity.

[1]Center for Space Physics, Boston University, Boston, Massachusetts, USA.
[2]Atmospheric Sciences, Haystack Observatory, Massachusetts Institute of Technology, Westford, Massachusetts, USA.

When large rocket engines burn above ~200 km, the exhaust gases are typically H_2, H_2O, and CO_2, and these species cause the F-layer O^+ and e^- to recombine about 1000 times faster than the normal loss rates due to ambient N_2 and O_2. Such rocket exhaust depletions (REDs) of the ionosphere were first detected using an ionosonde by the radiophysics pioneer Henry Booker [*Booker*, 1961]; they were then evaluated as an environmental impact concern by *Kellogg* [1964]. When measurements of TEC became possible, they were shown to display surprisingly large RED effects, even during daytime hours when photoionization was in progress [*Mendillo et al.*, 1975]. Theoretical studies and modeling were immediately initiated by *Bernhardt et al.* [1975]. Nighttime launches resulted in gradients ranging from 20 TEC units in 30 min to 50 TEC units in 2 min, depending on the relationship between the observing geometry and the rocket plume trajectory [*Mendillo et al.*, 1980; *Wand and Mendillo*, 1984]. Follow-up studies of chemically modified ionospheres as well-planned active experiments are described by *Bernhardt* [1987] and *Bernhardt et al.* [1988] and *Mendillo* [1988]. Here we report on the first case of a RED scenario detected by the GPS network over the eastern CONUS and, due to the postsunset launch time, its strong resemblance to the abrupt temporal passage of an SED phenomenon. That such "walls of depletion" capable of affecting the FAA and other users of GPS systems can occur suddenly, even though no geomagnetic storm was in progress, is the topic we address. While the storm time SED phenomenon has known spatial-temporal characteristics determined by geophysical causes, the RED gradient effects can occur along any possible launch trajectory and at any local time.

2. Observations

2.1. Plasma Signatures

[5] Figure 1 shows the launch trajectory that occurred on the night of 30 April 2005 when the U.S. Air Force launched a Titan IV B-30 rocket to an altitude of ~500 km. Of particular relevance is the spatial-temporal domain above 262 km where the exhaust rate from the second stage of the rocket introduced a total of 140 kg s^{-1} of TEC depleting chemicals (see Table 1). In Figure 2, we show the TEC maps over the eastern CONUS-Atlantic region during this time period that were generated from GPS receiving stations in the region. Figure 2 was derived using 862 stations, with data taken every 30 s. Each ground station can observe up to eleven satellites simultaneously, and from various directions, and thus data for the offshore region of interest come from stations along the U.S. east coast and in the Caribbean. The method of deriving TEC from GPS data, and the construction of regional TEC maps, has been fully described by *Rideout and Coster* [2006]. Shown here are maps constructed from 1-min averages of the standard Millstone Hill GPS TEC values, but with "empty pixels" filled by Delaunay interpolation and median-smoothed to the same resolution of optical airglow images to be shown. Figures 2a–2f are selected to show conditions just prior to launch and at four times during the onset and development of the effect. Figure 2f shows percent change from preevent conditions, a pronounced ~70% depletion in TEC. The ionosonde that operates routinely at Wallops Island, Virginia, observed the peak electron density to change from 3.8 to 1.1 × 10^5 e^-cm^{-3} during 0130–0200 UT (also a ~70% effect). An overflight of the area by a Defense Meteorological Satellite Program vehicle (DMSP F15) at 0200 UT showed a ~20% wall of depletion extending into the topside ionosphere (height = 840 km). Thus, all available diagnostics in the region showed a sudden, major perturbation to the ionosphere on this night. The pattern portrayed in Figure 2 is one clearly aligned (in space and time) along the launch trajectory given in Figure 1. The unusually severe transition from late afternoon TEC values to nighttime values is due unambiguously to known rocket exhaust induced chemistry and not, for example, to a naturally occurring enhanced decay rate of the ionosphere following sunset, nor to a dynamical effect a large-scale motions. Yet, from an operational perspective it is similar to the storm time case of an SED, except that during ionospheric storms the ambient ionosphere is first increased prior to its marked decline near dusk [*Mendillo et al.*, 1974; *Foster and Rideout*, 2005].

2.2. Optical Signatures

[6] As first pointed out by *Bernhardt et al.* [1975] and verified during the launch of an Atlas-F rocket [*Mendillo and Baumgardner*, 1982], the recombination chemistry that results in the rocket exhaust depletion of TEC also leaves many of the newly formed neutral oxygen atoms in excited states. Those in the $O(^1D)$ state emit photons at 6300 Å, and thus wide-angle imaging of the oxygen redline can be used to capture the onset and evolution of the chemical processes creating the depletions. That is, a burst of airglow occurs while a RED in TEC is forming. When the chemistry ends, so does the 6300 Å emission, but the effect in TEC endures until solar photoionization can replenish the *F* layer. For the daytime launch of a Saturn V rocket, the largest-ever RED in TEC was observed (spanning ~1 million square kilometers), and it took ~4 h of photoionization to recover [*Mendillo et al.*, 1975], with severe gradients for both onset and recovery. For a nighttime launch, as we have here, the depletion can last until the following sunrise period [*Mendillo et al.*, 1980].

[7] Figure 3 gives a visual picture of the causative RED scenario on this night. These data came from the Boston University all-sky camera that operates routinely at the Millstone Hill site. The launch occurred after sunset (LT = UT − 5 h), and shadow heights are 200 km or greater for all latitudes less than 36 degrees north. Thus, TEC replenishment by photo-ionization was not an important factor for the results in Figure 2. However, the ~2000 LT launch time was somewhat earlier than the normal starting time for optical observations, and thus extra care was taken in dealing with exposure times for the high sky-background

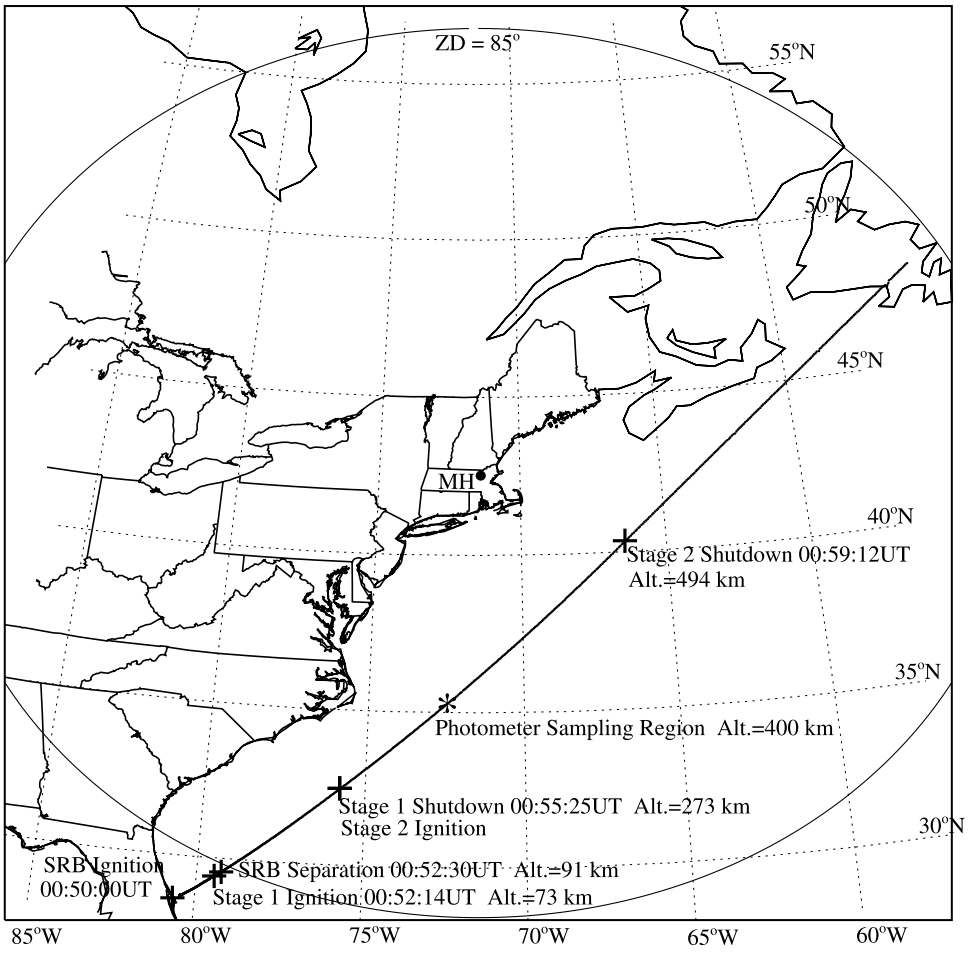

Figure 1. Map showing the trajectory of the Titan IV rocket launched from the Kennedy Space Center (KSC) at 0050 UT on 30 April 2005 (1950 LT at 75°W on 29 April). Plus symbols mark the times and heights when the solid rocket boosters (SRBs), first and second stages were ejecting exhaust gases into the atmosphere. The asterisk shows the point along the trajectory at 400 km where a time history of airglow emission and TEC depletions are portrayed in Figure 4.

levels. Figures 3a–3f result from standard all-sky image processing, as recently summarized by *Baumgardner et al.* [2007]. Basically, the background level was subtracted (about 1100 Rayleighs (R)) from preevent images, with calibration by a standard photometric C^{14} source. The fisheye view was ''unwarped'' to portray geographical space, assuming a constant emission height of 400 km (appropriate for the average entry point of exhaust as shown in Figure 1). The high background level is due to both the twilight conditions and the presence of thin cirrus clouds on this night. The confinement of the RED glow to latitudes equatorward of Millstone Hill is consistent with the launch sequence shown in Figure 1 and the TEC maps in Figure 2. Observations using the Millstone

Table 1. Rocket Engine and Exhaust Injection Parameters for the Titan IV B-30 Rocket Launch on 30 April 2005

Engine	Fuel and Oxidizer	Fuel Weight (kg)	Burn Period (UT)	Total Burn Time (s)	Exhaust Deposition Rate (kg s^{-1})	Burn Altitude Region (km)	Total Burn Region (km)
Stage 0 (SRB's)	HTPB	283,460	0050:00–0052:30	150	1890	0–91	91
Stage 1	N2H4/N2H2(CH3)2 and N2O4	140,600	0052:14–0055:25	191	736	73–273	200
Stage 2	N2H4/N2H2(CH3)2 and N2O4	31,750	0055:25–0058:47	227	140	273–494	221

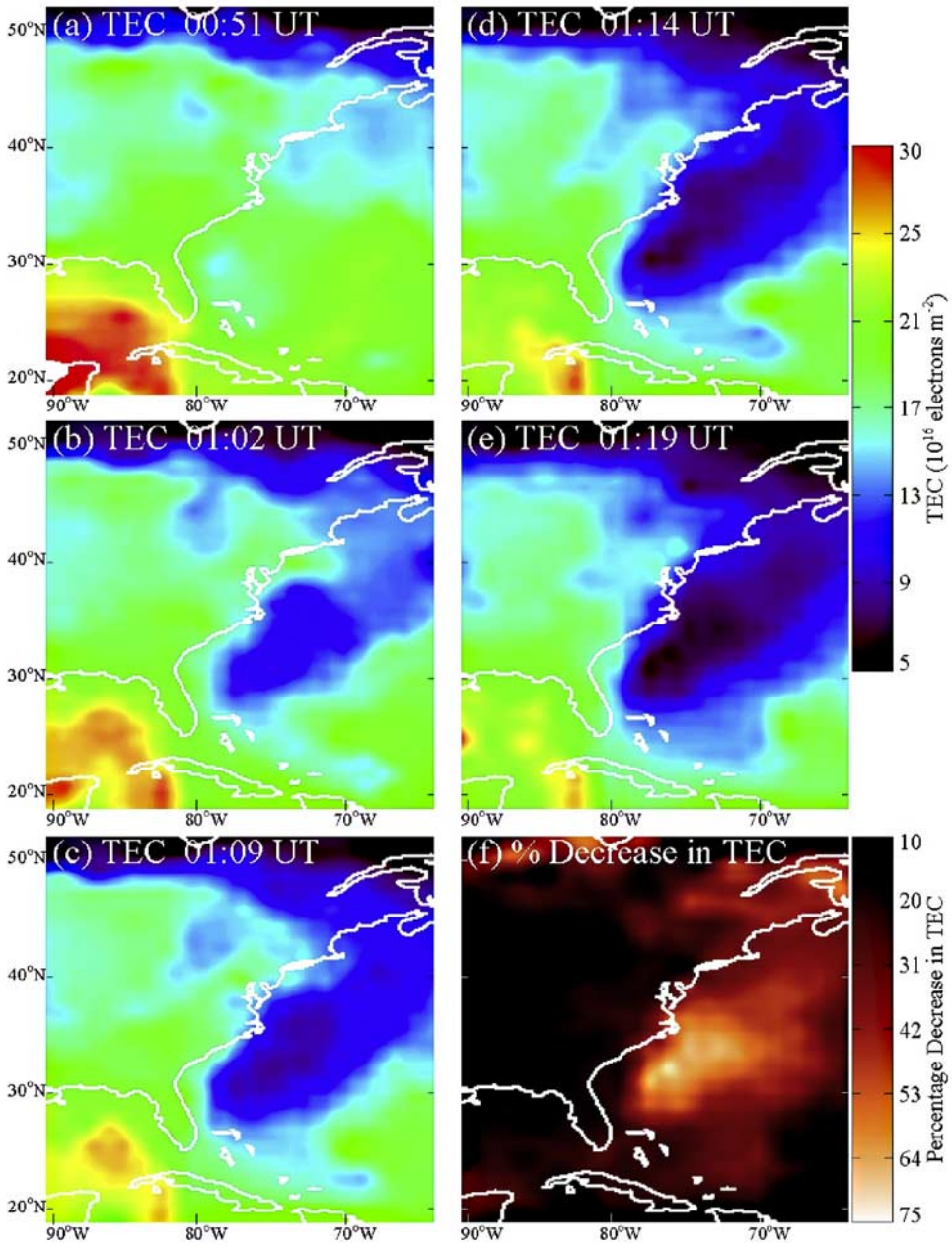

Figure 2. Maps of 1-min averages of total electron content (TEC) from the GPS network in the eastern United States at various times on 30 April 2005: (a) just after launch (0051 UT), (b) at 0102 UT, (c) at 0109 UT, (d) at 0114 UT and (e) at 0119 UT, all after engine shutdown (see Figure 1). (f) The percent differences between Figures 2a and 2e (see also the animation at http://www.buimaging.com/tec.html).

Hill incoherent scatter radar (ISR) on this night were limited to the vertical direction, and thus the nondetection of a perturbation by the ISR at 42.5°N is consistent with the spatial locations of the effects shown in Figures 2 and 3. Animations of the TEC maps showing original (pixel-by-pixel) data and the airglow images can be viewed at www.buimaging.com/tec.html.

[8] To illustrate the overall time history of the effect, Figure 4a shows the 6300 Å airglow brightness versus UT at the fixed location of 400 km along the rocket trajectory (34.58°N, 73.35°W), together with letters to serve as cross-

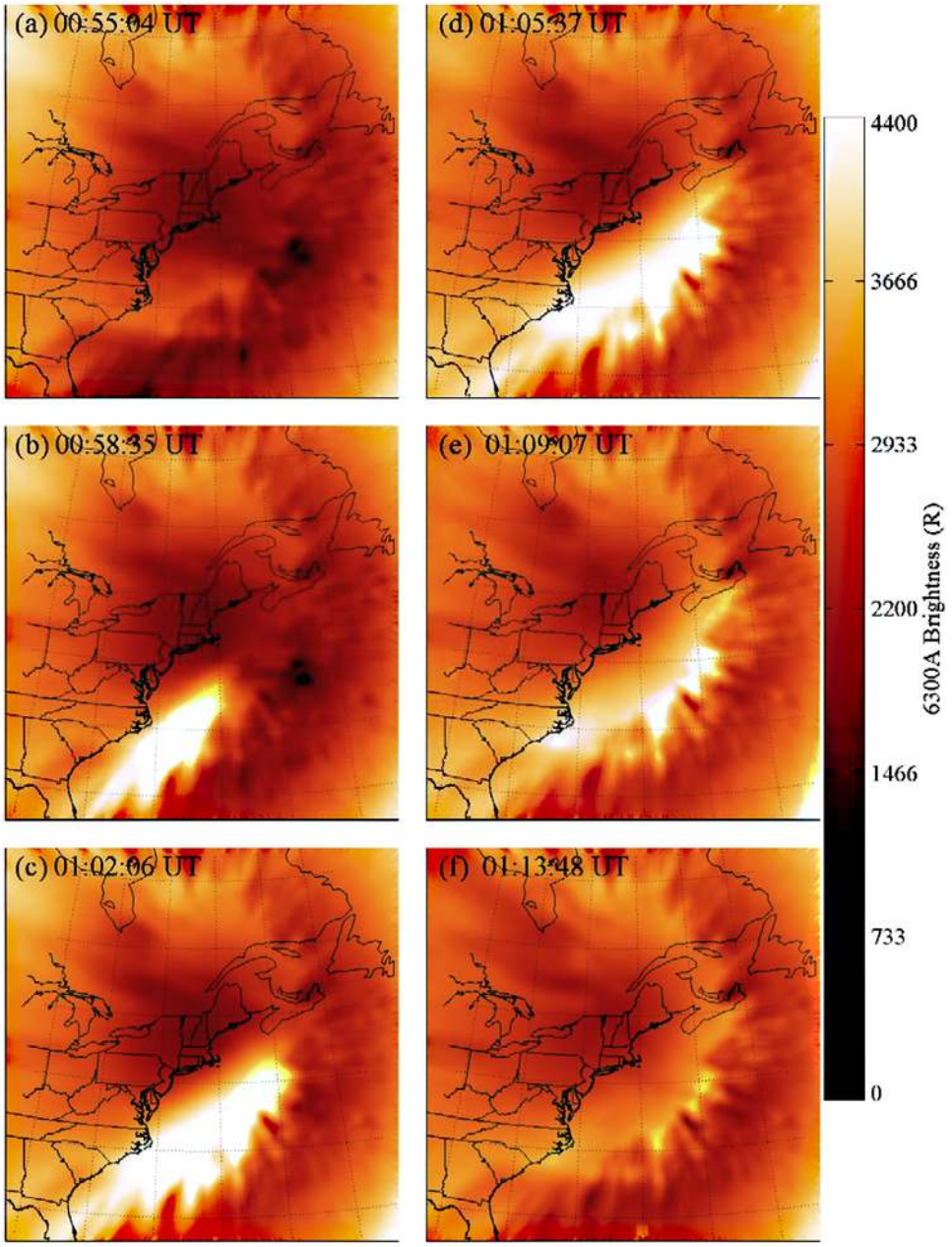

Figure 3. (a–f) The 6300 Å airglow generated by the rocket exhaust depletions (REDs) of TEC depicted in Figure 2. These optical maps were obtained using the all-sky camera at the Millstone Hill site in Westford, Massachusetts, for an average emission height of 400 km. Calibration is in brightness units of Rayleighs (R). The times in Figures 3c and 3e correspond to the TEC map times in Figures 2b and 2c, showing that the burst in airglow is a "formation-time" effect, while the TEC depletions are long-lived. The structured features in the south and southeast are due to trees at low elevation angles within the field-of-view from Millstone Hill (see also the animation at http://www.buimaging.com/tec.html).

references to the images in Figure 3. Figure 4b shows the change in TEC at that location, as determined by using the TEC values from the pixel closest to that point in the Millstone TEC maps. The somewhat earlier onset of the effect in TEC is due to exhaust gases from the second stage entering the lower ionosphere just prior to their massive entry into the airglow layer. The observed peak brightness of ~3.25 kR shown in Figure 3 has been corrected for

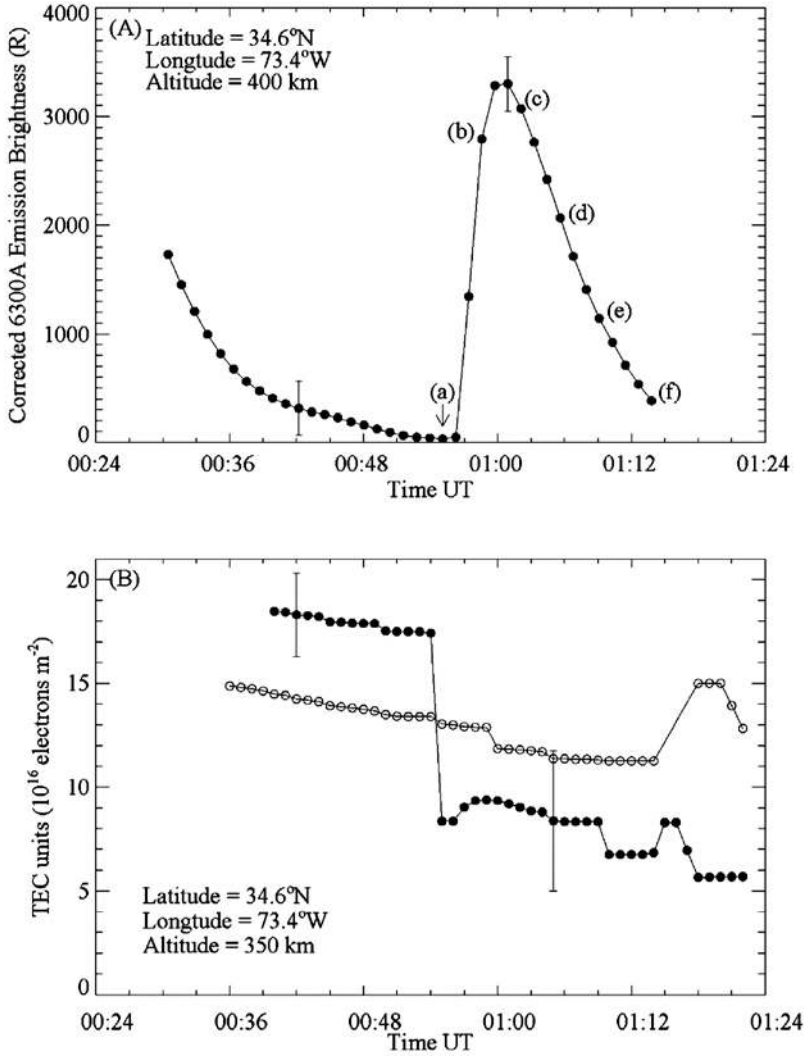

Figure 4. (a) The 6300 Å brightness in Rayleighs (R) obtained from the all-sky airglow images from Millstone Hill versus time at a fixed location (~34°N, ~73°W) with a line-of-sight altitude of 400 km along the rocket trajectory. The letters indicated refer to the panels in Figure 3. (b) The TEC pattern versus time at the same location (closed circles), shown in comparison to a control curve from the previous evening (open circles), as obtained from TEC maps on 29 and 30 April 2006. Uncertainty bars are shown for an individual 6300 Å image and an individual TEC 1-min value at preevent and postevent times.

atmospheric extinction and van Rhijn brightening. The total change in TEC of ~12 TEC units is essentially consistent with the relationship between these quantities found during pre-GPS events [*Mendillo and Baumgardner*, 1982].

3. Summary and Conclusions

[9] Ionospheric disturbances unrelated to solar-terrestrial activity can be caused by the introduction of large amounts of rocket exhaust into the thermosphere-ionosphere system. The effect is a sudden depletion of the ionospheric TEC that results in severe spatial gradients over a large region. Such rocket exhaust depletions (REDs) of TEC impact GPS signals used for navigation and position fixing in ways identical to those caused during large geomagnetic storms. Indeed, a brief loss of receiver lock was found for a few of the GPS records on this night, the very type of concern for aircraft navigation over CONUS that the FAA's wide area augmentation system (WAAS) needs to be aware of [*Doherty et al.*, 2004].

[10] The prediction of severe ionospheric gradients associated with naturally occurring ionospheric storm positive phase effects (i.e., SEDs) involves models of the full

solar terrestrial chain, the core activity of space weather researchers. For the NASA and DoD rocket launches that utilize high altitude engine burns from various launch sites (e.g., KSC in the east, White Sands and Vandenberg in the west), rocket exhaust depletion (RED) effects in TEC can also be predicted (i.e., the causative mechanism is well understood). Launch dates and times are usually known well in advance (with only a few launches classified). The geometries and times for severe TEC gradients due to a launch can therefore be predicted with considerable confidence. Yet, launches are often postponed for various reasons, so the alert system and monitoring program for RED effects can be quite different from those associated with geophysical causes. As shown here, however, even without prior planning the existing GPS network is well suited for real-time specification of the temporal and spatial domains affected by TEC RED events.

[11] **Acknowledgments.** Work on this study at Boston University was supported by grants from the Aeronomy Program and CEDAR Post-doctoral Program of the National Science Foundation (NSF). We thank Clara Narvaez for her assistance with analysis of the Wallops Island data and Ted Molczan (Toronto, Canada) for providing us with rocket coordinates and altitude data derived from Wallops Island radar tracking data. At Millstone Hill, funding for this study came from NSF grant ATM-0455831 and from support by the NSF cooperative agreement 0733510 with the Massachusetts Institute of Technology.

References

Baumgardner, J., J. Wroten, J. Semeter, J. Kozyra, M. Buonsanto, P. Erickson, and M. Mendillo (2007), A very bright SAR arc: Implications for extreme magnetosphere-ionosphere coupling, *Ann. Geophys.*, *25*, 2593–2608.

Bernhardt, P. A. (1987), A critical comparison of ionospheric depletion chemicals, *J. Geophys. Res.*, *92*, 4617–4628, doi:10.1029/JA092iA05p04617.

Bernhardt, P. A., C. G. Park, and P. M. Banks (1975), Depletion of the F2 region ionosphere and the protonosphere by the release of molecular hydrogen, *Geophys. Res. Lett.*, *2*, 341–344, doi:10.1029/GL002i008p00341.

Bernhardt, P. A., B. A. Kashiwa, C. A. Tepley, and S. T. Noble (1988), Spacelab 2 upper atmospheric modification experiment over Arecibo 1, Neutral gas dynamics, *Astrophys. Lett. Comm.*, *27*, 169–182.

Booker, H. (1961), A local reduction of the F region ionization due to missle transit, *J. Geophys. Res.*, *66*, 1073–1079, doi:10.1029/JZ066i004p01073.

Coster, A. J., J. C. Foster, P. J. Erickson, and R. J. Rich (2001), Regional GPS mapping of storm enhanced density during the 15–16 July 2000 geomagnetic storm, paper presented at ION GPS meeting, Inst. of Navig., Salt Lake City, Utah.

Coster, A. J., J. C. Foster, and P. J. Erickson (2003), Monitoring the ionosphere with GPS, *GPS World*, *14*(5), 42–45.

Davies, K. (1981), Review of recent progress in ionospheric predictions, *Radio Sci.*, *16*, 1407–1430, doi:10.1029/RS016i006p01407.

Doherty, P., A. Coster, and W. Murtagh (2004), Space weather effects of October–November 2003, *GPS Solut.*, *8*(4), 267–271, doi:10.1007/s10291-004-0109-3.

Foster, J. C., and W. Rideout (2005), Midlatitude TEC enhancements during the October 2003 superstorm, *Geophys. Res. Lett.*, *32*, L12S04, doi:10.1029/2004GL021719.

Kellogg, W. W. (1964), Pollution of the upper atmosphere by rockets, *Space Sci. Rev.*, *3*, 275–316, doi:10.1007/BF00180267.

Klobuchar, J. A., M. Mendillo, and F. L. Smith (1971), Ionospheric storm of March 8, 1970, *J. Geophys. Res.*, *76*, 6202--6207, doi:10.1029/JA076i025p06202.

Mendillo, M. (1988), Ionospheric holes: A review of theory and recent experiments, *Adv. Space Res.*, *8*(1), 51--62, doi:10.1016/0273-1177(88)90342-0.

Mendillo, M., and J. Baumgardner (1982), Optical signature of an ionospheric hole, *Geophys. Res. Lett.*, *9*, 215–218, doi:10.1029/GL009i003p00215.

Mendillo, M., and J. A. Klobuchar (1975), Investigations of the ionospheric F region using multistation total electron content observations, *J. Geophys. Res.*, *80*, 643–650.

Mendillo, M., and J. A. Klobuchar (2006), Total electron content: Synthesis of past storm studies and needed future work, *Radio Sci.*, *41*, RS5S02, doi:10.1029/2005RS003394.

Mendillo, M., J. A. Klobuchar, and H. Hajeb-Hosseinieh (1974), Ionospheric disturbances: Evidence for the contraction of the plasmasphere during severe geomagnetic storms, *Planet. Space Sci.*, *22*, 223–236, doi:10.1016/0032-0633(74)90026-9.

Mendillo, M., G. S. Hawkins, and J. A. Klobuchar (1975), A sudden vanishing of the ionospheric F region due to the launch of Skylab, *J. Geophys. Res.*, *80*, 2217–2228, doi:10.1029/JA080i016p02217.

Mendillo, M., D. Rote, and P. A. Bernhardt (1980), Preliminary report on the HEAO hole in the ionosphere, *Eos Trans. AGU*, *61*, 529–530.

Rideout, W., and A. Coster (2006), Automated GPS processing for global total electron content data, *GPS Solut.*, *10*(3), 219–228, doi:10.1007/s10291-006-0029-5.

Wand, R. H., and M. Mendillo (1984), Incoherent scatter observations of an artificially modified ionosphere, *J. Geophys. Res.*, *89*, 203–215, doi:10.1029/JA089iA01p00203.

J. Baumgardner, C. Martinis, M. Mendillo, and S. Smith, Center for Space Physics, Boston University, Boston, MA 02215, USA. (mendillo@bu.edu)

A. Coster and P. Erickson, Atmospheric Sciences, Haystack Observatory, Massachusetts Institute of Technology, Westford, MA 01886, USA.